NSERC CANRIMT
Canadian Network for Research and Innovation in Machining Technology
Réseau Canadien de recherché et d'innovation sur les technologies d'usinage

Joint Dynamics Identification on a Vertical CNC Machine

M. Mehrpouya[a], M. Law[b], C. Park[a], S. Park[a,*] and Y. Altintas[b]
[a]*Department of Mechanical & Manufacturing Engineering*
University of Calgary, Calgary, AB, Canada
[b]*Department of Mechanical Engineering*
University of British Columbia, Vancouver, BC, Canada
* *simon.park@ucalgary.ca*

Abstract: Accurate virtual machine tool models minimize the need for costly and time consuming physical trials before eventual physical prototyping. Design of accurate machine tools requires modeling of the joint dynamics between the tool and tool holder as well as between the tool holder and the spindle. To obtain the joint dynamics at these interfaces, we have formulated the inverse receptance coupling (IRC) which identifies the joint dynamics. This method enables us to combine analytical models with the experimental dynamics. The effectiveness of the IRC method is examined on a real three axis vertical CNC machining center. First, the finite element (FE) model of the holder and the tool along with the measured frequency response functions (FRFs) of the free-free holder–tool assembly are used to find the joint's dynamic properties between the holder and the tool. Secondly, a validated FE model of the machine tool is employed in the IRC method to obtain the joint's dynamic properties between the holder and the spindle using the measured receptances on the overall assembled structure. The verification has been performed with different cutting tools. The identified joint dynamics can be saved for particular joint conditions and used in future analysis of the virtual models.
Keywords: CNC Machine, Joint Identification, Receptance Coupling.

1. INTRODUCTION

Virtual prototyping facilitates exploration of several design alternatives to yield an optimal design, thus eliminating the need for costly and time consuming physical trials [Altintas *et al*., 2005]. This requires the virtual models to be accurate. The accuracy and efficacy of virtual machine tool models are strongly dependent on the joint characteristics; i.e. the stiffness and damping of the connections between various machine tool elements. Dynamic stiffness at the tool center point (TCP) of machine tools which governs the productivity of the process and the quality of the machined component is severely affected by the connections between the tool and tool-holder and between the tool-holder and the spindle. These connections are generally difficult to

model in the virtual environment with finite element codes and result in deviations between the virtual model and their corresponding physical prototypes, Figure 1.

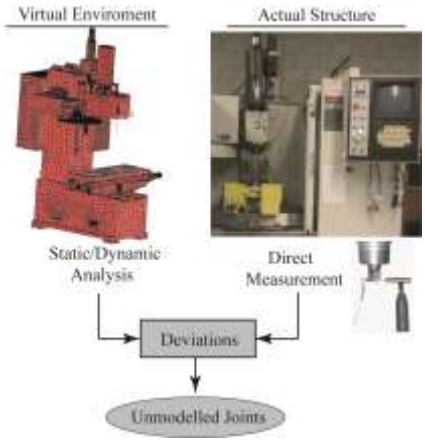

Figure 1; Effects of unmodeled joint.

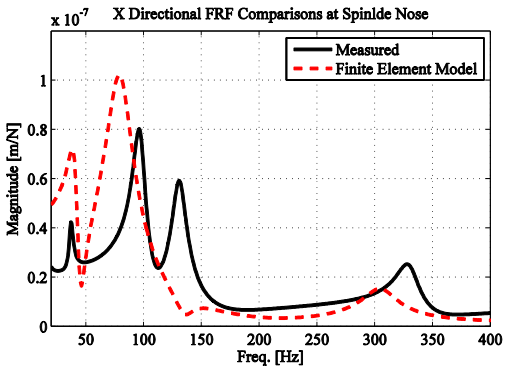

Figure2; Spindle nose FRF.

Several studies have therefore focused to address identification of joint dynamics based on direct and/or indirect methods. Direct methods requiring direct measurements at the joints are impractical due to the inaccessibility of the joints in the assembled structures. Hence, indirect methods of identification through the modal and receptance-based approaches find favour. In the modal approach, joint parameters are considered as uncertain parameters to be identified by minimizing the difference between the modal parameters, natural frequencies and mode shapes, of theoretical and experimental models [Mottershead *et al.*, 1993]. However, this method requires exact extraction of modal information, and slight variation in the mode shapes can result in erroneous results. To avoid difficulties of modal extraction, response based methods such as the receptance coupling (RC) approach are used. The RC method couples experimentally or analytically obtained frequency response functions (FRFs) and derives the response of the assembled structure. The RC method has been successfully employed to couple the receptances of different machine components and obtain FRFs at the TCP [Schmitz *et al.*, 2000; Park *et al.*, 2003; Erturk *et al.*, 2006]. In an inverse procedure through the inverse receptance coupling (IRC) method, the dynamics of the assembled structure and subcomponents are employed to obtain the joint properties between different substructures.

In this paper, the IRC method is used on a real structure to identify the joint dynamics between the holder and spindle and between the holder and the tool. The identification technique directly uses the measurements on the assembled structure which have valuable information about damping properties of the structure. In order to avoid measuring rotational receptances which is very challenging and difficult, only translational FRFs of the assembled structures are used in the identification. For the substructures, both rotational and translational FRFs are extracted from FE models and used in the identification.

2. VIRTUAL MACHINE TOOL MODEL

The machine tool is modeled based on a two stage substructural assembly approach. At first, each of the major substructures of the machine under consideration, namely: spindle-spindle-housing, column, base, cross-slide, and table are modeled independently and synthesized subsequently together with the three individual feed drive models. A second stage substructural assembly involves coupling the tool-tool-holder response to the response obtained at the spindle nose from the first stage using the RC approach. This allows different tool-tool-holder combinations to be modeled independently and coupled subsequently without having to regenerate machine (spindle) models [Schmitz *et al.*, 2000]. FE models for the structural substructures are generated from their respective CAD models using ten node solid tetrahedron elements with material properties assigned as: modulus of Elasticity of 89 GPa; density of 7250 kg/m^3; and, Poisson's ratio of 0.25. The spindle, three ball-screw drive models and the tool-tool-holder are modeled with Timoshenko beam elements. The spindle assembly including the spindle shaft, cartridge, bearings, drive pulley, and other accessories such as nuts and rotary couplings are modeled as described in [Law *et al.*, 2012]. The connections between all major substructures and between the spindle-spindle housing are assumed to be rigid.

To assess the accuracy of the virtual model, simulated spindle nose FRFs updated with modal damping are compared with measured fitted FRFs in Figure 2. The differences between the dynamic stiffness of the low frequency modes as well as order mismatch between the number of measured and simulated modes may be attributed to modeling simplifications in representing the machine accessories like the automatic tool changer and cabinets by lumped mass elements. Seeing that the virtual model is able to reasonably approximate the physical machine, joint identification between the tool-holder and the spindle and between the tool and tool-holder is treated in the next sections to better approximate the dynamic stiffness at the TCP.

3. JOINT IDENTIFICATION

The identification process in this paper is done through the IRC method. Firstly, the IRC method is used to find the joint dynamics between the holder and the tool by using two sets of measurements on the free-free holder-tool assembly. The identified joints are then used to build the model of the holder-tool assembly which is subsequently used to identify joint dynamics between the holder and the spindle. The identification at this step is performed by using the measured receptances along the tool while the holder-tool assembly was inserted inside the spindle.

3.1. Inverse receptance coupling (IRC)

Let Substructures A and B be connected through the joint which is comprised of rotational and translational elements as shown in Figure 3. Points *nA* and *nB* represent the internal locations on Substructures A and B, and, points *cA* and *cB* illustrate the

DOFs connected through the joint section. F_{nA}, F_{cA}, F_{nB}, F_{cB} are the forces in the assembled structure applied on the internal and connecting nodes in Substructures A and B, respectively.

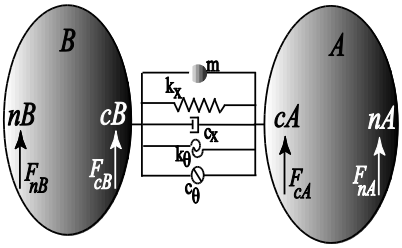

Figure 3; Subcomponents.

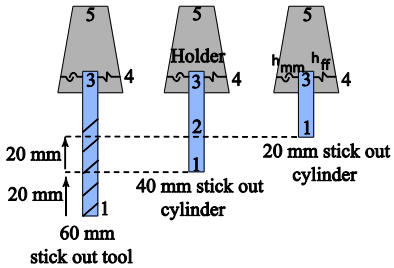

Figure 4; Tool-holder assemblies.

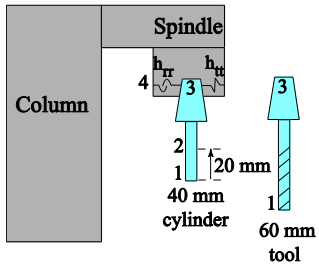

Figure 5; Spindle, holder, tool assemblies.

The relations between the displacements and the forces in each substructure are defined as:

$$\begin{Bmatrix} x_n^S \\ \theta_n^S \\ x_c^S \\ \theta_c^S \end{Bmatrix} = \begin{bmatrix} h_{nn}^S & l_{nn}^S & h_{nc}^S & l_{nc}^S \\ n_{nn}^S & p_{nn}^S & n_{nc}^S & p_{nc}^S \\ h_{cn}^S & l_{cn}^S & h_{cc}^S & l_{cc}^S \\ n_{cn}^S & p_{cn}^S & n_{cc}^S & p_{cc}^S \end{bmatrix} \begin{Bmatrix} f_n^S \\ M_n^S \\ f_c^S \\ M_c^S \end{Bmatrix} \tag{1}$$

where x_i^S and θ_i^S, ($S = A, B$; $i = n, c$), represent the translational and rotational displacement vectors at location i on Substructures A and B; and, $F_i^S = \{f_i^S , M_i^S\}$ represents the vector of force and moment. The receptance components are defined as $h_{ij}= x_i/f_j$, $l_{ij}= x_i/M_j$, $n_{ij}= \theta_i/f_j$ and $p_{ij}= \theta_i/M_j$.

The equilibrium condition at the joint part is: $\{f_J^A , M_J^A\}^T+ \{f_J^B , M_J^B\}^T = 0$, where $F_J^S = \{f_J^S , M_J^S\}$ is the vector of force and moment in the joint section at the connecting locations to Substructure S. Using the equilibrium conditions, the equation of motion at the joint part can be written as:

$$\begin{Bmatrix} x_c^A - x_c^B \\ \theta_c^A - \theta_c^B \end{Bmatrix} = \begin{bmatrix} h_{tt}^J & 0 \\ 0 & h_{rr}^J \end{bmatrix} \begin{Bmatrix} f_J^A \\ M_J^A \end{Bmatrix} = \begin{bmatrix} k_x + ic_x\omega & 0 \\ 0 & k_\theta + ic_\theta\omega \end{bmatrix}^{-1} \begin{Bmatrix} f_J^A \\ M_J^A \end{Bmatrix} = [H_J] \begin{Bmatrix} f_J^A \\ M_J^A \end{Bmatrix} \tag{2}$$

where H_J denotes the receptance matrix of the joint and subscripts t and r represent the translational and rotational directions, respectively. Considering that forces and displacements of the internal co-ordinates do not change before and after coupling, the assembled structure's FRFs can be obtained by substituting Eq. 1 into Eq. 2 [Park *et al.*, 2003]. Considering that two internal locations are available for the measurements on a structure, $nA = \{1, 2\}$, and naming the connecting points on Substructures A and B as $cA = 3$ and $cB = 4$, two assembled structure's FRFs are expanded as:

$$G_{11,tt} = \frac{x_1}{f_1} = h_{11} - \frac{1}{b_{tt}b_{rr} - b_{rt}b_{tr}}[(h_{12}b_{rr} - l_{12}b_{rt})h_{21} + (-h_{12}b_{tr} + l_{12}b_{tt})n_{21}]$$

$$G_{12,tt} = \frac{x_1}{f_2} = h_{12} - \frac{1}{b_{tt}b_{rr} - b_{rt}b_{tr}}[(h_{12}b_{rr} - l_{12}b_{rt})h_{22} + (-h_{12}b_{tr} + l_{12}b_{tt})n_{22}] \tag{3}$$

$$, \begin{bmatrix} b_{tt} & b_{tr} \\ b_{rt} & b_{rr} \end{bmatrix} = \begin{bmatrix} h_{33} & l_{33} \\ n_{33} & p_{33} \end{bmatrix} + \begin{bmatrix} h_{44} & l_{44} \\ n_{44} & p_{44} \end{bmatrix} + \begin{bmatrix} h_{tt}^J & 0 \\ 0 & h_{rr}^J \end{bmatrix}$$

where $G_{ij,tt}$ represents the assembled structure's translational FRFs. To find the joint FRFs, h_{tt}^{J} and h_{rr}^{J}, Eq.3 is solved simultaneously in the MATLAB® symbolic toolbox; and, the explicit solutions for the joint's FRFs are derived as:

$$h_{tt}^{J} = \frac{\left(b_{rt}G_{12,tt}h_{31} - b_{rt}h_{12}h_{31} - b_{rt}G_{11,tt}h_{32} + b_{rt}h_{11}h_{32} - h_{13}h_{32}n_{31} + h_{13}^{2}n_{32}\right)}{G_{12,tt}l_{13} - h_{12}l_{13} - G_{11,tt}l_{23} + h_{11}l_{23}} - h_{33} - h_{44}$$

$$h_{rr}^{J} = \frac{\left(b_{tr}G_{12,tt}n_{31} - b_{tr}h_{12}n_{31} + h_{32}l_{13}n_{31} - b_{tr}G_{11,tt}n_{32} + b_{tr}h_{11}n_{32} - h_{31}l_{13}n_{32}\right)}{G_{12,tt}h_{31} - h_{12}h_{31} - G_{11,tt}h_{32} + h_{11}h_{32}} - p_{33} - p_{44} \quad (4)$$

Based on Eq. 4, the joint FRFs are related to the assembled structure's translational receptances, which are found experimentally, and the substructures' FRFs, which are obtained through the FE model. This eliminates the dependence of identification on the rotational FRF measurements and gives an explicit solution for the joint FRFs.

Equation 4 will be frequently used in the identification of joint dynamics in the following sections. At each identification stage, two measured receptances along with the FE models of substructures are used to find the joint's FRFs. In order to assess the accuracy of identified joint's FRFs, different tools are inserted in the holder and the identified joint FRFs are used in Eq. 3 to build the new assembled structure's FRFs. The reconstructed FRFs are then compared with the directly measured FRFs on the new structure.

3.2. Joint identification between holder and tool

The experimental setup in this section included a CAT40 tool-holder, two cylinders, 50 mm and 70 mm long, and one actual end mill, 90 mm long, which were each inserted 30 mm inside the holder, Figure 4. These components were all modeled with Timoshenko beam elements in the FE environment. The translational as well as rotational FRFs at locations H_{44} and H_{45} on the tool-holder were obtained from its FE model. The cylinder/ tool FRFs, H_{11}, H_{12}, H_{22} and H_{13} were also obtained from the corresponding FE models.

For identification of the joint between the shank of 40 mm cylinder and the holder, two measurements were performed at locations 1 and 2 on the assembled structure, in Figure 4, with the holder-tool in free-free configuration, i.e. with unsupported conditions. This information, along with the FRFs of the holder and the cylinder were inserted into Eq. 4 to find the translational and rotational FRFs of the joint – shown in Figures 6 and 7 respectively.

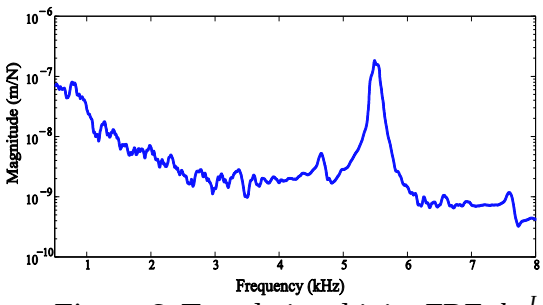

Figure 6; Translational joint FRF, h_{tt}^{J}.

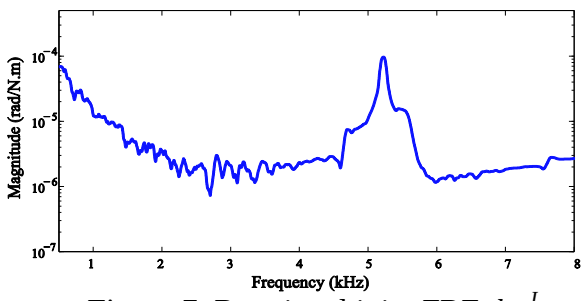

Figure 7; Rotational joint FRF, h_{rr}^{J}.

The structural modes of the joint are observed to be between 5 kHz to 6 kHz. If the dynamics of a structure which uses this holder-tool setup is sought around these frequencies, i.e. 1-10 kHz, the effects of the joint between the holder and the tool cannot be ignored. To investigate the accuracy of the identified joint FRFs, and, the potential improvements in the assembled structure FRFs resulting from the joint FRFs, the FRFs for the 20 mm cylinder and 60 mm tool were reconstructed by inserting the identified joint's FRFs and substructures' FRFs in Eq. 3. The reconstructed FRFs are compared with the measured FRFs on the corresponding free-free assemblies in Figures 8 and 9.

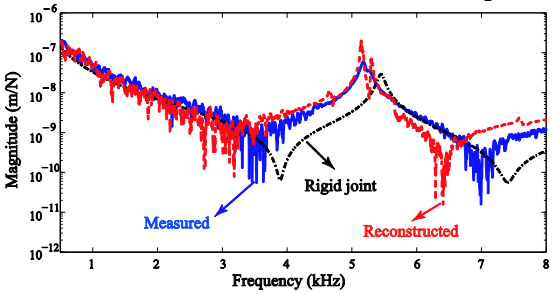

Figure 8; Direct FRFs with Holder-tool, G_{11_20mm}.

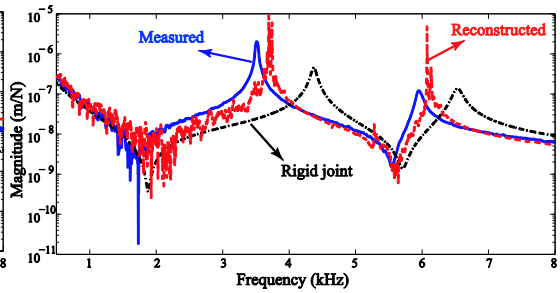

Figure 9; Direct FRFs with Holder-tool G_{11_60mm}.

Based on Figures 8 and 9, a considerable improvement in the prediction of the holder-tool assembly was obtained with identified joint dynamics compared to the rigid joint connection. The error in prediction of first two consecutive natural frequencies has improved from 24.0% and 9.7% in the rigid joint assumption to 5.0% and 2.1% in the reconstructed FRF, Figure 9. When this holder-tool assembly is inserted inside the spindle, the interface between these two bodies influences the dynamics at the TCP. The joint at this interface is identified in the next section.

3.3. Joint identification between spindle and holder

Two substructures are considered in this section: a FADAL 2216 machine tool whose response at the spindle nose was obtained from the virtual model in Section 2 and, the holder-tool whose mathematical model was built by considering the joint effects between holder and tool. The identification procedure was done when the 40 mm cylinder-holder assembly, Figure 5, was inserted inside the spindle. Two measurements were done along the cylinder, one at the cylinder tip and one 20 mm away from the tip, to obtain the $G_{11,tt}$ and $G_{12,tt}$ FRFs. These FRFs along with the FRFs at the spindle nose, H_{44}, Figure 5, and the FRFs for the holder-cylinder assembly, H_{11}, H_{12}, H_{13}, H_{23} and H_{33}, were inserted into Eq. 4 to obtain the joint's translational and rotational FRFs, h_{tt}^{J} and h_{rr}^{J}. Figure 10 shows the translational joint's FRF and several structural modes exist in the joint FRF. This shows that the joint between the holder and the spindle has more significant effects on the dynamics of the assembled structure than the joint between the tool and holder, which showed only one structural mode.

To further validate the accuracy of the identified joint properties, the joint's FRFs were used to build the tool tip FRFs for the 60 mm tool–holder assembly. To do this, the 40 mm cylinder-holder assembly was replaced with the 60 mm tool-holder assembly.

The spindle nose FRFs, H_{44}, the tool-holder FRFs, H_{11}, H_{13}, in Figure 5, and the joint's FRFs, h^J_{tt} and h^J_{rr}, were inserted into Eq. 3 to find TCP FRFs. Figure 11 shows the comparison between the reconstructed FRF, measured FRF at the tip of 60 mm tool and the assembled FRF obtained by considering a rigid joint between the holder and spindle, $h^J_{tt} = h^J_{rr} = 0$ in Eq. 3. Based on Figure 11, a close prediction was obtained for the tip FRFs compared to the measured FRFs.

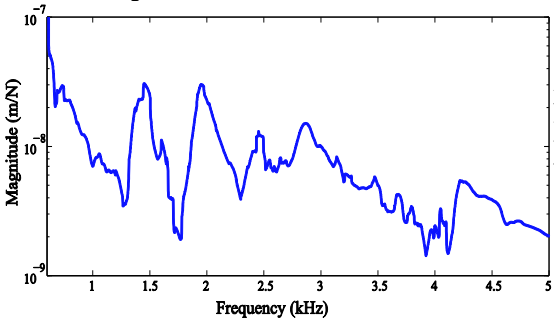

Figure 10; Translational Joint FRF between Spindle and holder, h_{tt}^J.

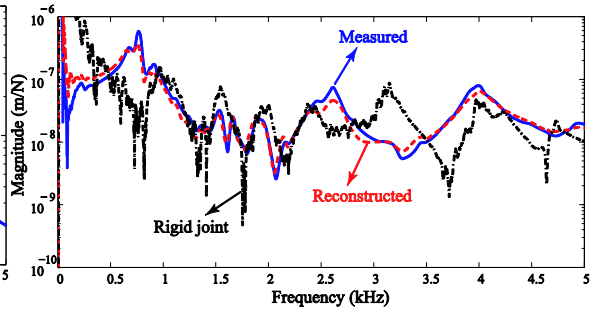

Figure 11; Direct FRF at TCP with Spindle-holder-tool, G_{11_60mm}.

The considerable improvements that were obtained in predicting the tip FRFs compared to the rigid joint approximation showed the importance of the joint dynamics properties both between the holder and the tool and between the holder and the spindle. If an accurate prediction at the TCP is sought, the joint dynamics effects should be taken into account at both places. The proposed method in this study had several assumptions and limitations in the modeling, experiments and simulations. First, the off-diagonal terms in the FRF matrix are assumed to have negligible effects on the assembled structure FRFs. This assumption is true if, as in this study, the joint section mainly acts as a connecting element and imposes stiffness and damping to the structure. The behaviour of the joint was also considered to be linear in the studied frequency range, so the friction was modeled with a linear viscous damping element and nonlinear effects such as slipping were ignored [Ibrahim *et al.*, 2005]. The behaviour of the joint was also considered to be time-invariant and stable.

Secondly, since the measured data was convoluted with the noise, a Savitzky–Golay filter [Orfaidis 1996] was applied to the recorded signals before analysis. This helped us to prevent error magnification while dealing with the matrix inversion in the identification step. From the modeling point of view, differences between the measured and simulated response at the spindle nose will compound inaccuracies in the identification since simulated rotational FRFs are used in place of difficult to measure experimental FRFs. Idealization of cylinders and tools with Timoshenko beam models may have also caused some deviations in the identified joint properties. Lastly, the accuracy of the identified joint dynamics and their validity depend on similarity of joint conditions in the identification and validations structures. Many conditions such as contact area, pre-stress and manufacturing tolerances can affect the joint behaviour. The proposed methods are applicable when the influential conditions on the joint's dynamic behaviour remain constant after replacing different substructures.

4. CONCLUSIONS

In this paper, the inverse receptance coupling method was applied on an actual three axis CNC machine to identify the joint characteristics between the tool & the holder, and between the holder & the spindle. The complete virtual (FE) model of the machine tool was first validated and synthesized with the FE models of holder and tools.

First, the joint between the tool and the holder was identified and used to improve the mathematical model of the holder-tool assembly. The holder-tool model was then synthesized with the FE model of the spindle to obtain the joint properties between the holder and the spindle. A considerable improvement in response prediction for the assembled structure was observed by modeling and identifying the joint dynamics as compared to treating the joint as rigid. The identified joint properties can be incorporated into the virtual model of the actual machine to improve its accuracy and decrease the deviation between its prediction and actual behaviour of the structure. Further studies are required to incorporate the effects of applied pre-stress and tool diameter on the identified properties.

ACKNOWLEDGEMENT
The authors acknowledge the funding support of NSERC CANRIMT for this work.

REFERENCES

[Altintas et al., 2005] Altintas, Y.; Brecher, C.; Weck, M.; Witt, S.; “Virtual machine tool”; *CIRP Annals*, 54, pp. 651-674; 2005.

[Schmitz et al. 2000] Schmitz, T.L.; Donaldson, R.; “Predicting high-speed machining dynamics by substructure analysis”; *CIRP Annals*, 49, pp.303-308; 2000.

[Park et al. 2003] Park, S.S.; Altintas, Y.; Movahhedy, M.R.; “Receptance coupling for end mills”; *Journal of Machine Tools & Manufacture*, 43, pp. 889-896; 2003.

[Erturk et al. 2006] Erturk, A.; Ozguven, H.N.; Budak, E.; “Analytical modeling of spindle-tool dynamics on machine tools using Timoshenko beam model and receptance coupling for the prediction of tool point FRF”, *Journal of Machine Tools & Manufacture*, 46, pp. 1901-1912; 2006.

[Law et al. 2013] Law, M.; Phani, A.S.; Altintas, Y.; “Position-dependent multibody dynamic modeling of machine tools based on improved reduced order models”, *Journal of Manufacturing Science and Engineering, Vol. 135, 2013*.

[Ibrahim et al. 2005] Ibrahim, R.A.; Pettit, C.L.; “Uncertainties and dynamic problems of bolted joints and other fasteners”, *Journal of Sound &Vibrations*, 279, pp. 857-936; 2005.

[Orfaidis 1996] Orfaidis, S.J.; “Introduction to Signal Processing”, Prentice-Hall, New Jersey, 1996.

[Mottershead et al. 1993] Mottershead, J.E.; Friswell, M.I.; “Model updating in structural dynamics: a survey”; *Journal of Sound and Vibration*, 167, pp. 347–375; 1993.